JPP
Journal of
Pharmacy and Pharmacology

JPP 2010, 62: 709–720

Received October 29, 2009
Accepted January 11, 2010
DOI 10.1211/jpp/62.06.0007
ISSN 0022-3573

Research Paper

Transdermal iontophoretic delivery of a novel series of dopamine agonists *in vitro*: physicochemical considerations

Oliver W. Ackaert[a], Jeroen De Graan[b], Romano Capancioni[a], Durk Dijkstra[b], Meindert Danhof[c] and Joke A. Bouwstra[a]

[a]Division of Drug Delivery Technology and [c]Division of Pharmacology, Leiden/Amsterdam Center for Drug Research, Leiden and [b]Department of Medicinal Chemistry, University Center of Pharmacy, University of Groningen, Groningen, the Netherlands

Abstract

Objectives The transdermal iontophoretic delivery of a novel series of 2- aminotetralins and chromanamine-based dopamine agonists was investigated *in vitro*.

Methods Systematic structural modifications allowed us to investigate their effect on solubility in the donor phase and iontophoretic delivery across human skin. Transport profiles were analysed with nonlinear mixed effect modelling, utilizing an extension to an existing compartmental model. Furthermore, relationships between physicochemical properties and transport parameters were addressed.

Key findings A solubility increase was observed: 5,6-di-OH-DPAT < 5-OH-MPAT < 5-OH-EPAT < 8-OH-DPAC. The structure significantly affected the iontophoretic delivery across human stratum corneum and dermatomed human skin with the highest flux for 5-OH-EPAT and 5-OH-MPAT. The extended model with two skin release constants (K_{R1}, K_{R2}) described more adequately iontophoretic transport profiles than the existing model with one release constant. The extended model suggested two parallel transport pathways during current application. Across human stratum corneum, the electrophoretic mobility, measured with capillary electrophoresis, showed a linear relationship with the electromigrative flux and the zero-order iontophoretic mass input into the skin (I_0).

Conclusions Combining transport parameters (I_0, K_{R1} and K_{R2}), predicted from physicochemical properties, with compartmental modelling provided a powerful tool to simulate iontophoretic transport profiles for screening potential candidates and designing experiments.

Keywords dopamine agonists; iontophoresis; modelling; transdermal; transport pathway

Introduction

Transdermal iontophoresis enhances the delivery of small charged solutes across the skin by application of a small current (≤ 0.5 mA/cm^2) across this membrane. Important advantages of transdermal delivery are circumvention of the hepatic first-pass effect and a continuous administration of the drug. A particular advantage of iontophoresis is the possibility to adjust the rate of delivery by changing the current density.[1] For the symptomatic treatment of Parkinson's disease the current strategy is to administer therapeutic agents in a continuous manner to reduce the induction of motor fluctuations after long-term use.[2–4] Most of the dopamine agonists have a very narrow therapeutic window, which demands for an accurate individualized titration, adjusted to the needs of the therapy.[5,6] For these reasons, the in-vitro and in-vivo iontophoretic delivery of dopamine agonists, such as apomorphine, ropinirole, 5-OH-DPAT and rotigotine, have been investigated intensively.[7–16]

To improve the transport efficiency and consequently the therapeutic treatment of Parkinson's disease, a good understanding is required about the structure–transport relationship. However, with respect to this class of drugs little is known about the structure–transport relationship. In this study, the in-vitro iontophoretic delivery of a new series of dopamine agonists, which were selected based on their potency and their molecular structure, has been investigated.[17–23] The small structural differences allowed us to investigate in detail the influence of molecular structure and related physicochemical properties of the dopamine agonists on the iontophoretic transport efficiency.

Correspondence: Joke A. Bouwstra, Division of Drug Delivery Technology, Leiden/Amsterdam Center for Drug Research, Einsteinweg 55, 2333 CC Leiden, The Netherlands.
E-mail: bouwstra@lacdr.leidenuniv.nl

Over the years several studies have focused on selecting the key physicochemical properties that determine the efficiency of transdermal iontophoretic delivery. It has been reported that the size of the solute, expressed as molecular weight (MW) or molecular volume (MV), is an important descriptor with a higher transport for smaller molecules.[24–26] Furthermore, an increase in charge/MW ratio resulted in an increase in transdermal electromigrative flux, as was observed for a series of peptides.[27] In a follow up study by Abla *et al.*[28] the electrophoretic mobility, measured by capillary zone electrophoresis, provided an estimation of the electromigrative flux. Finally, the lipophilicity of the transported molecules also affected the transdermal iontophoretic transport, however the relationship with the corresponding transport efficiency was not as straightforward as with passive diffusion.[29,30]

Most of these physicochemical property–transport relationships use a single parameter to describe the transdermal iontophoretic flux. As a single end-point the flux at the end of the iontophoresis period or the steady-state flux and lag time are often selected. However, in these approaches, the information on the shape of the iontophoresis transport curve is neglected, which makes extrapolation towards the in-vivo situation more difficult. The mathematical models introduced by Nugroho *et al.*[16,31,32] were designed to overcome the aforementioned disadvantages and to make the extrapolation from the in-vitro to in-vivo transport studies more reliable. The proposed models were based on a commonly used assumption for iontophoresis, namely a constant mass input into the skin during iontophoresis due to the constant iontophoretic driving force resulting from the application of a constant current. An adapted model, based on the compartmental models introduced by Nugroho *et al.*,[16,31] has been presented and applied to describe the iontophoretic flux profile for this series of dopamine agonists. In this study the relationship between the physicochemical properties and the transport has been addressed, using the electromigrative flux as single end-point and using the adapted model describing the total iontophoretic flux profile.

The objectives of this study were: to investigate the transdermal iontophoretic delivery *in vitro* of a new series of dopamine agonists; to evaluate the adapted mathematical compartmental model to describe the in-vitro iontophoretic delivery of these dopamine agonists; and to study the relationships between the physicochemical properties (clogP, electrophoretic mobility and MW) of the molecules and the electromigrative flux (EM-flux) and the parameter estimates (zero-order mass input from donor to skin and skin release constants), using the adapted model.

Materials and Methods

Materials

The 2-aminotetralins 5-hydroxy-2-(N-ethyl,N-n-propylamino) tetralin (5-OH-EPAT.HBr), 5-hydroxy-2-(N-n-propylamino) tetralin (5-OH-MPAT.HBr), 5,6-di-hydroxy-2-(N-n-propylamino)tetralin (5,6-di-OH-MPAT.HBr), 5,6-di-hydroxy-2-(N,N-di-n-propylamino)tetralin (5,6-di-OH-DPAT.HBr), 5-hydroxy-2-(N,N,-di-n-propylamino)tetralin (5-OH-DPAT. HBr) and the chromanamine 8-hydroxy-3-(N,N,-di-n-propylamino)chroman (8-OH-DPAC.HBr) (Figure 1; purity > 95%, determined with HPLC and NMR) were synthesized at the Department of Medicinal Chemistry of the University of Groningen, Groningen, The Netherlands. Silver, silver chloride (purity > 99.99%), trypsin (type III from bovine pancreas) and trypsin inhibitor (type II-S from soybean) were obtained from Sigma-Aldrich (Zwijndrecht, The Netherlands). Paracetamol (acetaminophen) was purchased from Brocacef BV (Maarssen, The Netherlands) and D-Mannitol was obtained from BDH Laboratory supplies (Poole, UK). Spectra/Por RC dialysis membrane disks (cut-off value of 6000–8000 Da) were purchased from Spectrum Laboratories, Inc (Rancho Dominquez, CA, USA). Tetrahydrofuran (THF, stabilized, purity > 99.8%) was obtained from Biosolve (Valkenswaard, The Netherlands). Triethylamine (TEA, purity > 99%) was obtained from Acros Organics (Geel, Belgium). All other chemicals and solvents were of analytical grade. All solutions were prepared in Millipore water with a resistance of more than 18 MΩ/cm.

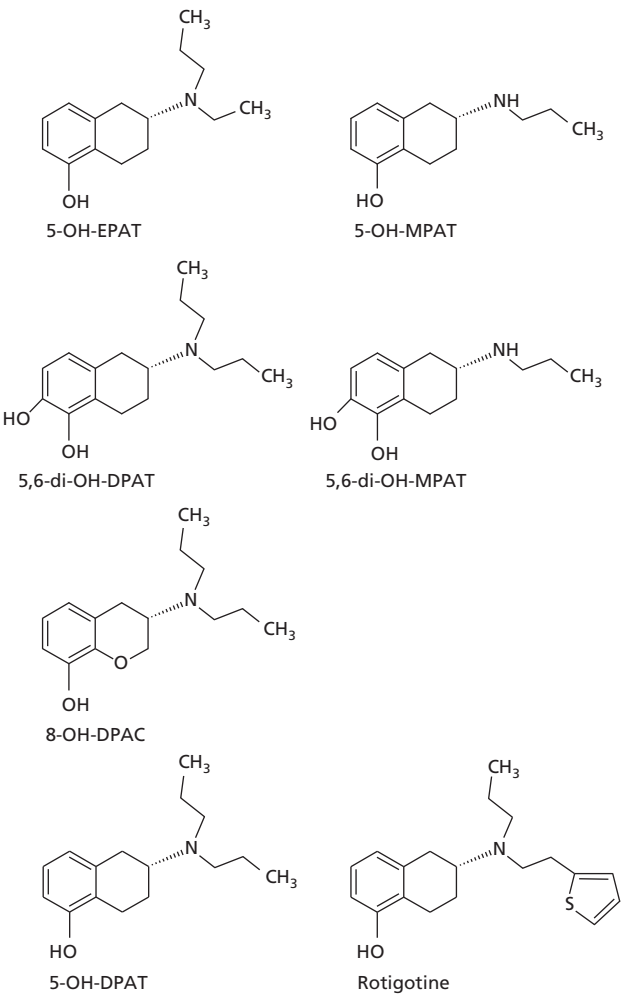

Figure 1 The chemical structures of different dopamine agonists

Maximum solubility

The solubility studies of the different compounds were carried out as described elsewhere.[14] Briefly, each compound was solubilized in citric buffer 5 mM, pH 5 + 4 g/l NaCl + 23.1 g/l D-mannitol. Subsequently the pH in each test tube was adjusted to pH 5 with 1 M NaOH or 1 M HCl under continuous shaking. Each solution was shaken for 48 h, after which the solution was centrifuged and filtered. The concentration in each solution was determined with HPLC.

Stability of 5,6-di-OH-MPAT and 5,6-di-OH-DPAT

The oxidation of 5,6-di-OH-MPAT and 5,6-di-OH-DPAT was investigated under various conditions. At the starting point 0.1 mg/ml 5,6-di-OH-DPAT and 5,6-di-OH-MPAT were dissolved in the buffer solution. The solutions were continuously stirred and kept constant at the desired temperature, using a thermostat-controlled water bath. If required a circular sheet of human stratum corneum (ø = 18 mm) was added to the solution and a current of 320 μA was applied. At regular intervals samples were taken from the solution and diluted in Millipore water, containing 2.86% v/v antioxidant solution (0.5% w/v ascorbic acid 0.05% w/v EDTA and 25% v/v H_3PO_4) to prevent the molecule from oxidizing further. The amount of remaining drug was quantified by RP-HPLC (see Analytical methods).

Capillary electrophoresis

Previous studies have shown that the electrophoretic mobility at 7.4 was related to the iontophoretic mobility during transdermal transport.[28,33] The electrophoretic mobility of various compounds in this study was investigated with capillary electrophoresis. These experiments were performed using an HPCE system (model number: G1600OAX, Agilent Technologies Santa Clara, CA, USA) equipped with an on-column diode-array detector, an autosampler, and a 30 kV power supply. Capillary electrophoresis Chemstation (Agilent Technologies) was used for capillary electrophoresis control, data acquisition and handling. The separation was performed in a 50-μm fused-silica capillary 48.5 cm in total length, and 40 cm to the UV detector. All experiments were carried out in cationic mode (the anode at the inlet and cathode at the outlet). The concentration of the samples was 0.5 mM in water and dimethyl sulfoxide (DMSO) in water (0.5% v/v) was added to the solution as a marker for the electroosmotic flow. The electrophoretic mobility was determined using a phosphate buffer pH 7.4 (Na_2HPO_4 5.82 g/l; NaH_2PO_4 5.1 g/l) as electrolyte solution (mobile phase). UV detection was applied at 220 and 278 nm for the detection of DMSO and the molecule, respectively. The capillary was preconditioned as follows: 5 min 0.1 M NaOH + 10 min electrolyte solution. The sample was injected over 5 s under a pressure of 50 mbar. Every sample was measured three times and for every analysis a fresh electrolyte solution was used. The effective electrophoretic mobility (μ_{eff}) was calculated as follows:

$$\mu_{eff} = \mu_{obs} - \mu_{EOF} = \frac{L_{tot} L_{eff}}{V}\left[\left(\frac{1}{t_{obs}}\right) - \left(\frac{1}{t_{EOF}}\right)\right] \qquad (1)$$

with μ_{obs} and μ_{EOF} as the electrophoretic mobility of the compound and the electroosmotic marker DMSO, respectively. L_{tot} and L_{eff} are the total distance of the capillary and the distance from the inlet to the detection point, respectively. t_{obs} and t_{EOF} are the time required to reach the detection point for the analyte and the electroosmotic marker DMSO, respectively, and V is the applied voltage.[34,35]

In-vitro transport studies

The preparation of dermatomed human skin and human stratum corneum was performed according to a method described previously.[15] All transport experiments were carried out as described elsewhere.[15] The donor formulation (citric buffer 5 mM, pH 5, NaCl 4 g/l, D-mannitol 23.1 g/l), containing the solute, was added to the anodal chamber. The cathodal chamber was filled with phosphate-buffered saline (PBS; pH 7.4, NaCl 8 g/l, Na_2HPO_4 2.86 g/l, KH_2PO_4 0.2 g/l, KCl 0.19 g/l). The acceptor phase, maintained at 32°C, was continuously perfused with PBS pH 7.4 at a flow rate of 7.0 ml/h. The following protocol was used: 6 h passive diffusion + 9 h iontophoresis (500 μA/cm²) + 5 h passive diffusion. Samples were collected every hour with an automatic fraction collector (ISCO Retriever IV, Beun De Ronde BV, Abcoude, The Netherlands). The specific conditions of the individual transport studies are described below. To prevent oxidation of 5,6-di-OH-DPAT and 5,6-di-OH-MPAT after transdermal transport and before analysis, 200 μl antioxidant solution (EDTA (Titriplex III): 0.5 g/l, $Na_2S_2O_5$ 5 g/l, H_3PO_4 (85 wt % in H_2O) 294 ml/l) was added to every collecting tube in the fraction collector.

Total iontophoretic flux

The iontophoretic delivery of 5-OH-EPAT, 5-OH-MPAT, 5,6-di-OH-MPAT and 5,6-di-OH-DPAT and 8-OH-DPAC across human stratum corneum was studied at 3.9 mM. Two additional concentrations (1.5 and 7.0 mM) of 5-OH-EPAT and 5-OH-MPAT were studied. For 5-OH-EPAT, 5-OH-MPAT, 5,6-di-OH-DPAT, 5-OH-DPAT and 8-OH-DPAC, transport studies across dermatomed human skin were performed using a donor concentration of 3.9 mM.

Electroosmotic flux

According to the Nernst-Planck equation the total flux (J_{tot}) consists of three transport mechanisms:

$$J_{Tot} = J_{EM} + J_{EO} + J_P \qquad (2)$$

with the electromigrative flux (J_{EM}) and the electroosmotic flux (J_{EO}) as the principal driving mechanisms for iontophoresis of charged species. The passive flux (J_P) is often negligible. The electroosmotic flux across human stratum corneum was investigated during iontophoretic transport of 5-OH-EPAT, 5-OH-MPAT, 5,6-di-OH-DPAT and 8-OH-DPAC (3.9 mM). Paracetamol (15 mM) was added to the donor phase as a marker for the electroosmotic flux. The electroosmotic flux was calculated, using the following equation, assuming a similar electroosmotic transport for the analogues and paracetamol:

$$J_{EO} = \frac{J_{par}}{C_{par}} x C_m \qquad (3)$$

with J_{par} as the flux of paracetamol and C_m and C_{par} as the donor concentration of the molecule and paracetamol, respectively.

Compartmental modelling

The iontophoretic transport *in vitro* of different molecules was analysed using nonlinear mixed effects modelling. The starting point of the models was a zero-order mass transport from the donor solution into the skin during and after iontophoresis. In this study an extension to the basic model has been presented.

Basic model in vitro

An extensive explanation and description of the basic model is presented elsewhere.[31] Briefly, the basic model assumes a constant rate of mass input from the donor into the skin during iontophoresis due to a constant iontophoretic driving force. Based on this assumption the equations to describe in-vitro iontophoretic transport during (eqn 4) and after current application (eqn 6) are:

$$J(t) = \frac{I_0}{S}(1-e^{-K_R.(t-t_L)}) \quad (4)$$

$$J_{ss} = \frac{I_0}{S} \quad (5)$$

$$J(t) = \frac{P_{PI}}{S}(1-e^{-K_R.(t-T)}) + \frac{I_0}{S}(1-e^{-K_R.(T-t_L)}).e^{-K_R(t-T)} \quad (6)$$

where $J(t)$ is the flux at time t and S is the diffusion area, K_R is a first-order skin release rate constant, I_0 is the zero-order iontophoretic mass transfer from the donor compartment into the skin compartment during current application, t_L is the kinetic lag time parameter, introduced to address the time required for drug molecules to enter the skin compartment, T is time of current application, J_{ss} is the flux at steady state and P_{PI} is the zero-order drug input due to the passive driving force post-iontophoresis.

Extended model in vitro

As observed from the iontophoretic flux profile of the compounds presented in this paper, the flux increased in time during the current application. This suggested that two transport routes were involved in the iontophoretic delivery, linked in parallel. The observed flux is the total amount of drug released in the acceptor compartment. In analogy to the basic model the zero-order mass transfer from the donor into the skin remains constant, however the first-order release constant from the skin to the acceptor will be different for both transport mechanisms. Therefore the iontophoretic flux *in vitro* during iontophoresis ($t \leq T$) can be described by the equation:

$$J(t) = \frac{I_0}{S}(1-e^{-K_{R1}.(t-t_L)}) + \frac{I_0}{S}(1-e^{-K_{R2}.(t-t_L)}) \quad (7)$$

$$J_{ss} = 2 * \frac{I_0}{S} \quad (8)$$

with K_{R1} and K_{R2} as the release constants to describe both transport routes. During the post-iontophoresis period ($t > T$) only one release constant appeared to be sufficient to describe the passive flux, resulting in the following equation:

$$J(t) = \frac{P_{PI}}{S}(1-e^{-K_{R2}.(t-T)}) + \left(\frac{I_0}{S}(1-e^{-K_{R1}.(T-t_L)}) + \frac{I_0}{S}(1-e^{-K_{R2}.(T-t_L)})\right).\ e^{-K_{R2}(t-T)} \quad (9)$$

Curve fitting and model evaluation

Fitting the data was performed using the subroutines ADVAN6 TOL = 5 from PREDPP in NONMEM (NONMEM version VI). Interindividual variability was modelled using an exponential error model and the residual error was characterized by an exponential and/or additive error model. The estimation of the population parameters was performed using a conventional first-order method.[36]

The extended model was evaluated in comparison with the basic model. The statistical analysis was based on the objective function, which is defined as 2-times the logarithm of the likelihood. If the objective function of the extended model with two release constants during the current application decreases with a value of 4 (or more) compared with the objective function of the basic model, the extended model is significantly better ($P < 0.05$; Chi-square test).

Analytical method

Different HPLC methods were developed to analyse the respective molecule and paracetamol by RP-HPLC. The aminotetralins and the chromanamine were detected using a scanning fluorescence detector (Waters 474, Millipore, Milford, MA, USA) and paracetamol was detected using a UV detector (Dual λ Absorbance Detector 2487, Waters, Milford, USA). The column, the composition of the mobile phase, the volume of injection and the respective excitation and emission wavelengths to analyse the different compounds are depicted in Table 1. The flow rate was set to 1.0 ml/min. Calibration curves showed a linear response between 100 and 40 000 ng/ml ($r^2 > 0.99$). The limit of detection (LOD) and limit of quantification (LOQ) for these HPLC methods can also be found in Table 1.

Data analysis

All data are presented as mean ± standard deviation (SD) or as mean ± standard error of the mean (SEM). When a statistical analysis was performed comparing only two groups, a Student's *t*-test was used. When three or more groups were compared, a one-way analysis of variance was executed. Comparing the effect of two factors simultaneously was performed using two-way analysis of variance. If the overall P value was less than 0.05, a Bonferonni post-test was applied to compare different groups. Statistical tests were performed by using GraphPad Prism version 5.00 for Windows (GraphPad Software, San Diego, CA, USA). For all statistical analysis a significance level of $P < 0.05$ was used.

Table 1 The HPLC method used for the various 2-aminotetralins and chromanamine-based dopamine agonists investigated

Compound	Column	Mobile phase			Fluorescence			
		Composition (% v/v)	TEA (mM)	injection volume (μl)	λ_{ex} (nm)	λ_{em} (nm)	LOD (ng/ml)	LOQ (ng/ml)
5-OH-EPAT	Superspher RP-select B C8	Ace 50 mM/THF 95/5	30	20	275	302	21.0	35.0
5-OH-MPAT	Inertsil5 ODS-2	Ace 100 mM/ACN 90/10	15	50	280	310	8.2	12.3
5,6-di-OH-DPAT	Superspher RP-select B C8	Ace 50 mM/THF 97/3	15	200	276	305	61.4	115.9
5,6-di-OH-MPAT	Inertsil5 ODS-2	Ace 50 mM/THF 96/4	15	50	280	310	90.7	150.5
8-OH-DPAC	Superspher RP-select B C8	Ace 50 mM/THF 95 / 5	30	50	277	306	29.9	44.9
Paracetamol	a							

[a]Mobile phase, column, limit of detection (LOD) and limit of quantification (LOQ) are dependent on the compound co-analysed; UV-detection, λ = 243 nm. λ_{em}, emission wavelength; λ_{ex}, excitation wavelength; Ace, acetate buffer pH 3.6; ACN, acetonitrile; TEA, triethylamine; THF, tetrahydrofuran.

Results

Maximum solubility

The maximum solubility of the different compounds was determined in citric buffer 5 mM at pH 5 in the presence of 68 mM NaCl and D-mannitol as this was the composition of the donor solution used for transport studies. The results of the solubility assay can be found in Table 2.[37–39] The solubility data of rotigotine.HCl and 5-OH-DPAT, adapted from the literature, were added to Table 2 for comparison. An increase in solubility was observed ranking the molecules in the following order: rotigotine < 5,6-di-OH-DPAT < 5-OH-DPAT < 5-OH-MPAT < 5-OH-EPAT < 8-OH-DPAC. Furthermore the relative hydrophilicity of the different analogues, expressed with the octanol–water partition coefficient, clogP, was calculated/computed using the ALOGPS 2.1 webservice.[37–39] The results are also provided in Table 2.

Stability of 5,6-di-OH-MPAT and 5,6-di-OH-DPAT

The catechol group of 5,6-di-OH-MPAT and 5,6-di-OH-DPAT was expected to be susceptible to photo-, auto- and chemical oxidation to ortho-semiquinone and subsequently to ortho-quinone, similar to apomorphine, another catecholamine.[41] Therefore the stability of these two molecules was investigated under various conditions, mimicking the different compartments during in-vitro iontophoretic transport. Figure 2, evaluating the % remaining catechol after 24 and 48 h, shows that 5,6-di-OH-MPAT remained stable at pH 5 at room temperature. Increasing only the temperature had little influence on the stability: after 48 h the remaining 5,6-di-OH-MPAT was 95.9 and 87.7 ± 5.6% at room temperature and 32°C, respectively. Addition of human stratum corneum and application of a current decreased the remaining drug from 96.2 ± 3.1 to 90.2% after 24 h. In analogy to other catecholamines, the pH of the solution had a strong influence on the stability of the two compounds.[41,42] At pH 5 5,6-di-OH-MPAT and 5,6-di-OH-DPAT were more stable than at pH 6. Increasing the pH to 7.4 resulted in an even more pronounced degradation of 5,6-di-OH-MPAT.

Capillary electrophoresis

To assess the electrophoretic mobility of the various compounds, capillary electrophoresis was performed (Table 2). The electrophoretic mobility of the various compounds increased in the following order: rotigotine < 5,6-di-OH-DPAT < 5,6-di-OH-MPAT < 8-OH-DPAC < 5-OH-DPAT < 5-OH-EPAT < 5-OH-MPAT.

Table 2 The physicochemical properties of the various 2-aminotetralins and chromanamine-based dopamine agonists investigated

	Compound	Molecular weight (g/mol)	clogP[c]	Solubility (mM)	Electrophoretic mobility (μ_{em}) × 10^{-4} (cm^2/s/V) ± SD
1	5-OH-EPAT	233.36	3.71	111.7	1.84 ± 0.01
2	5-OH-MPAT	205.30	2.93	93.1	1.88 ± 0.00
3	5,6-di-OH-DPAT	263.38	3.74	44.2	1.56 ± 0.01
4	5,6-di-OH-MPAT	221.30	2.5	ND	1.61 ± 0.01
5	8-OH-DPAC	249.36	3.4	282.5	1.64 ± 0.01
6	5-OH-DPAT	247.38	4.15	56.7[a]	1.76 ± 0.01
7	Rotigotine	315.48	4.82	7.1[b]	1.49 ± 0.04

The molecular weight and the calculated logP (clogP) are presented together with the solubility in a citric buffer 5 mM pH 5, containing 4 g/l NaCl and 23.1 g/l D-mannitol, and the electophoretic mobility, determined with capillary electrophoresis. The solubility of 5-OH-DPAT and rotigotine, obtained from literature, are added to the table for comparison. [a,b]Value adapted from literature.[14,40] [c]clogP was calculated using ALOGPS 2.1.[37–39] ND, not determined.

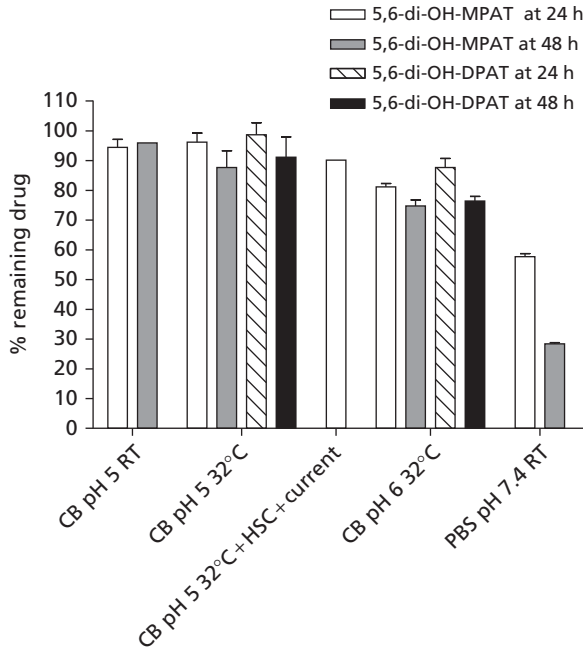

Figure 2 The amount of catechol remaining after time. Bar plot of the % remaining of 5,6-di-OH-MPAT and 5,6-di-OH-DPAT after 24 and 48 h under various conditions. The data are presented as mean ± SD, n = 2–3. CB, citric buffer; current = 320 μA; HSC, circular sheet of human stratum corneum (ø = 18 mm); PBS, phosphate-buffered saline; RT, room temperature

Iontophoretic transport

Total transport across human stratum corneum and dermatomed human skin

Transport studies with the dopamine agonists at 3.9 mM were performed to compare the iontophoretic delivery of the various compounds. The different flux profiles of the analogues across human stratum corneum and dermatomed skin are depicted in Figure 3a and b, respectively. The flux of the different compounds was evaluated statistically after 9 h of iontophoresis (current density was 500 μA/cm²). Across stratum corneum one-way analysis of variance showed an overall significant difference in the flux of the different compounds ($P < 0.0001$). The observed flux after 9 h increased in the following order: 5,6-di-OH-MPAT (134.5 ± 12.9 nmol/cm²/h) < 5,6-di-OH-DPAT (175.0 ± 15.9 nmol/cm²/h) < 8-OH-DPAC (175.9 ± 18.9 nmol/cm²/h) < 5-OH-DPAT (207.7 ± 38.0 nmol/cm²/h) < 5-OH-MPAT (219.7 ± 31.4 nmol/cm²/h) < 5-OH-EPAT (247.7 ± 12.1 nmol/cm²/h). In a follow up study two additional concentrations (1.5 and 7.0 mM) of 5-OH-MPAT and 5-OH-EPAT were investigated. Comparing the flux of 5-OH-MPAT and 5-OH-EPAT after 9 h of iontophoresis at 1.5 (99.6 ± 15.9 vs 68.7 ± 22.0 nmol/cm²/h), 3.9 mM (see above) and 7.0 mM (404.9 ± 72.9 vs 354.2 ± 78.1 nmol/cm²/h) showed no significant difference (two-way analysis of variance; $P > 0.05$) (Figure 3c). A similar trend was seen for iontophoretic transport studies across dermatomed skin: 8-OH-DPAC (168.2 ± 13.2 nmol/cm²/h) < 5,6-di-OH-DPAT (175.2 ± 25.9 nmol/cm²/h) < 5-OH-DPAT (193.0 ± 19.9 nmol/cm²/h) < 5-OH-EPAT (199.8 ± 8.0 nmol/cm²/h) < 5-OH-MPAT (241.8 ± 11.2 nmol/cm²/h). A significant difference could be observed between the fluxes of the different compounds (one-way analysis of variance; $P < 0.05$).

Electroosmotic contribution across human stratum corneum

Paracetamol (15 mM) was added to the donor solution to investigate the electroosmotic flow across human stratum corneum during iontophoretic transport. The resulting electroosmotic contribution, calculated using equation 3, expressed as % of the total flux, is depicted in Figure 4. A significantly higher electroosmotic contribution was observed when 5,6-di-OH-DPAT (12.1 ± 3.4%) was transported through stratum corneum, compared with the other compounds 5-OH-EPAT (4.5 ± 0.9%), 5-OH-MPAT (4.6 ± 1.4%) and 8-OH-DPAC (6.1 ± 0.4%) (one-way analysis of variance, Bonferroni post test; $P < 0.01$).

Model evaluation

The iontophoretic transport of the different compounds was fitted using the basic and extended model. The basic model assumes a constant input during iontophoresis with one skin release constant K_R. As an example the iontophoretic flux of 8-OH-DPAC (3.9 mM) across human stratum corneum is shown in Figure 5. The iontophoretic transport of 3.9 mM 8-OH-DPAC (open circle), together with the model predictions of the basic model (dashed line) clearly showed that the basic model did not fit to the experimental data. For this reason we employed the extended model with two release constants, K_{R1} and K_{R2}. The extended model described more adequately the flux of the drug than the basic model (Figure 5, solid line). This graphical analysis was performed for all compounds across dermatomed human skin and stratum corneum. The majority of the individual fits showed an improvement when using the extended model. The two models were also evaluated statistically by comparison of the objective function of the models. Except for rotigotine across dermatomed skin and 5,6-di-OH-MPAT across stratum corneum, in all cases the objective function decreased with a value larger than 4. This indicated that although an extra parameter (K_{R2}) was added to the model, a clear improvement in fitting the iontophoretic transport across human sttatum corneum and dermatomed skin was obtained ($P < 0.05$; Chi-square test). A model using two zero-order mass input rates (I_0) or an additional release constant (K_{R3}) did not improve data fitting.

Discussion

In this study, the transdermal iontophoretic delivery of a series of 2-aminotetralins and a chromanamine (8-OH-DPAC) has been presented. The systematic structural differences of these compounds allowed us to investigate the effect of molecular structure on the solubility and on iontophoretic delivery efficiency.

Solubility

The differences in structure affected the solubility of the various compounds greatly. Compared with 5-OH-DPAT, approximately a twofold higher solubility was observed for

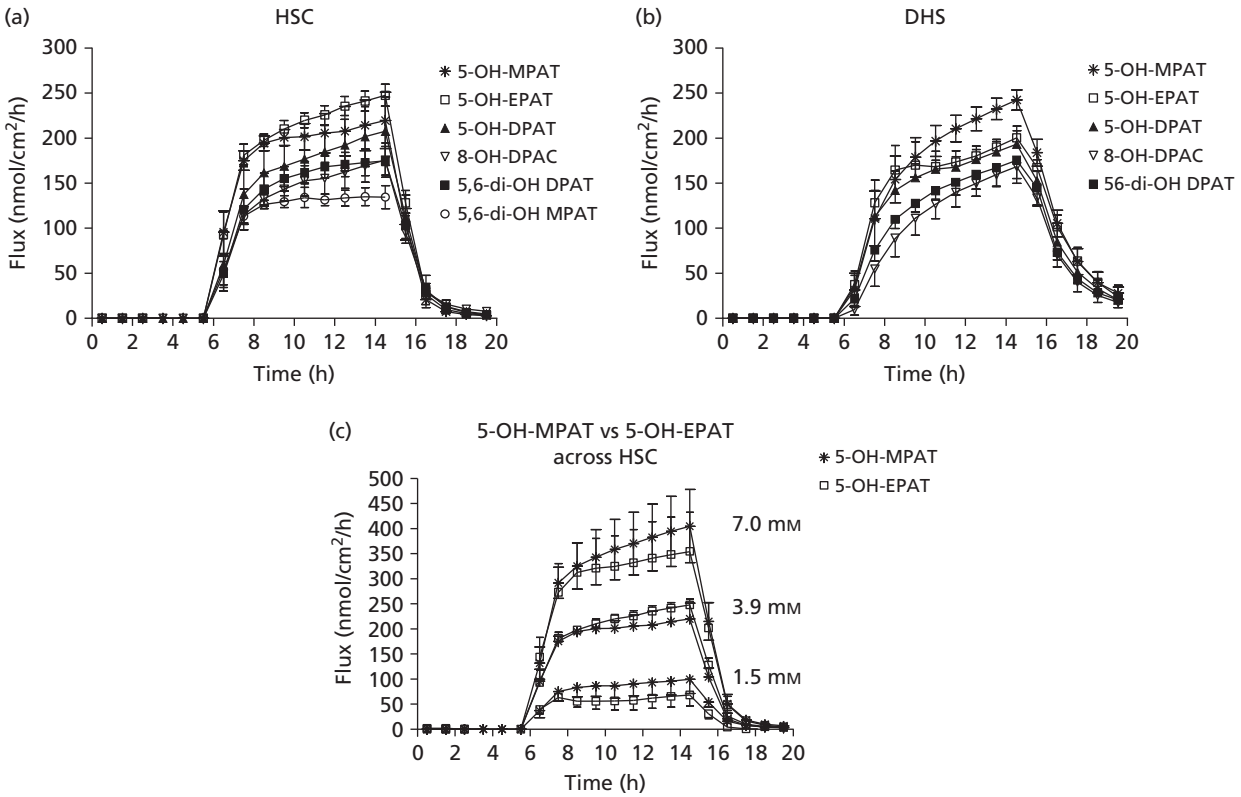

Figure 3 The iontophoretic flux profile of the different dopamine agonists across (a) human stratum corneum and (b) dermatomed human skin. The donor concentration of all the compounds was 3.9 mM. (c) The comparison of the iontophoretic flux vs time profile of 5-OH-MPAT and 5-OH-EPAT across stratum corneum at three different concentrations (1.5, 3.9, 7.0 mM). The data are presented as mean ± SD, $n = 4–7$. DHS, dermatomed human skin; HSC, human stratum corneum

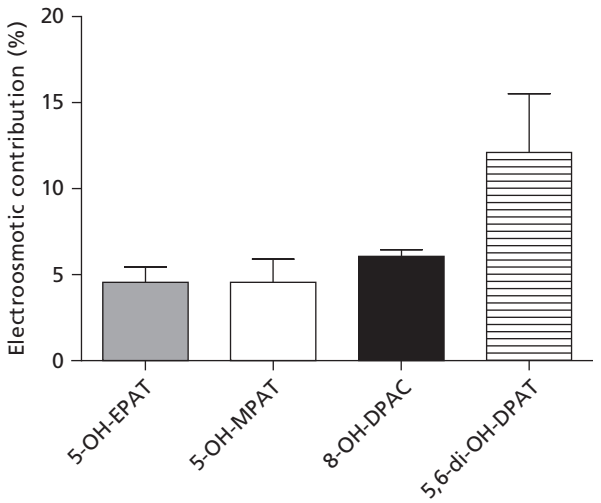

Figure 4 Electroosmotic contribution during iontophoretic transport of different compounds across human stratum corneum. The donor concentration was 3.9 mM. Paracetamol (15 mM) was co-transported to determine the electroosmotic flow during iontophoretic transport. The data are presented as mean ± SD, $n = 5–6$

5-OH-EPAT and 5-OH-MPAT, indicating that decreasing the length of the alkyl side chain on the nitrogen group improved the solubility of the compound, most probably due to reduction in lipophilicity and an increase in chargeability of the nitrogen group. Furthermore for 8-OH-DPAC almost a fivefold higher solubility was observed compared with 5-OH-DPAT. This demonstrated that replacement of the tetrahydronaphthalene moiety, present in the structure of 5-OH-DPAT, by a chroman moiety (as in 8-OH-DPAC) increased the solubility. In contrast, 5,6-di-OH-DPAT showed a reduced solubility, which could be explained by the formation of intermolecular hydrogen bridges, decreasing its water solubility.

Efficiency of iontophoretic transport

Small structural changes influenced the transport efficiency of the different analogues across human stratum corneum and dermatomed skin significantly. Although steady state had not been reached after 9 h of current application, a clear difference could be observed at this time point. Despite the increase in hydrophilicity of 5,6-di-OH-MPAT and 5,6-di-OH-DPAT by introducing an extra oxygen on the phenyl ring, the iontophoretic flux reduced, compared with 5-OH-MPAT and 5-OH-DPAT. It has been reported that an increase in molecular volume results in a decrease in total iontophoretic flux, but in an increase in electroosmotic contribution.[24,43] The significantly higher electroosmotic contribution for 5,6-di-OH-DPAT might have been due to an increased molecular volume, caused by intermolecular hydrogen bonds, which would also account for

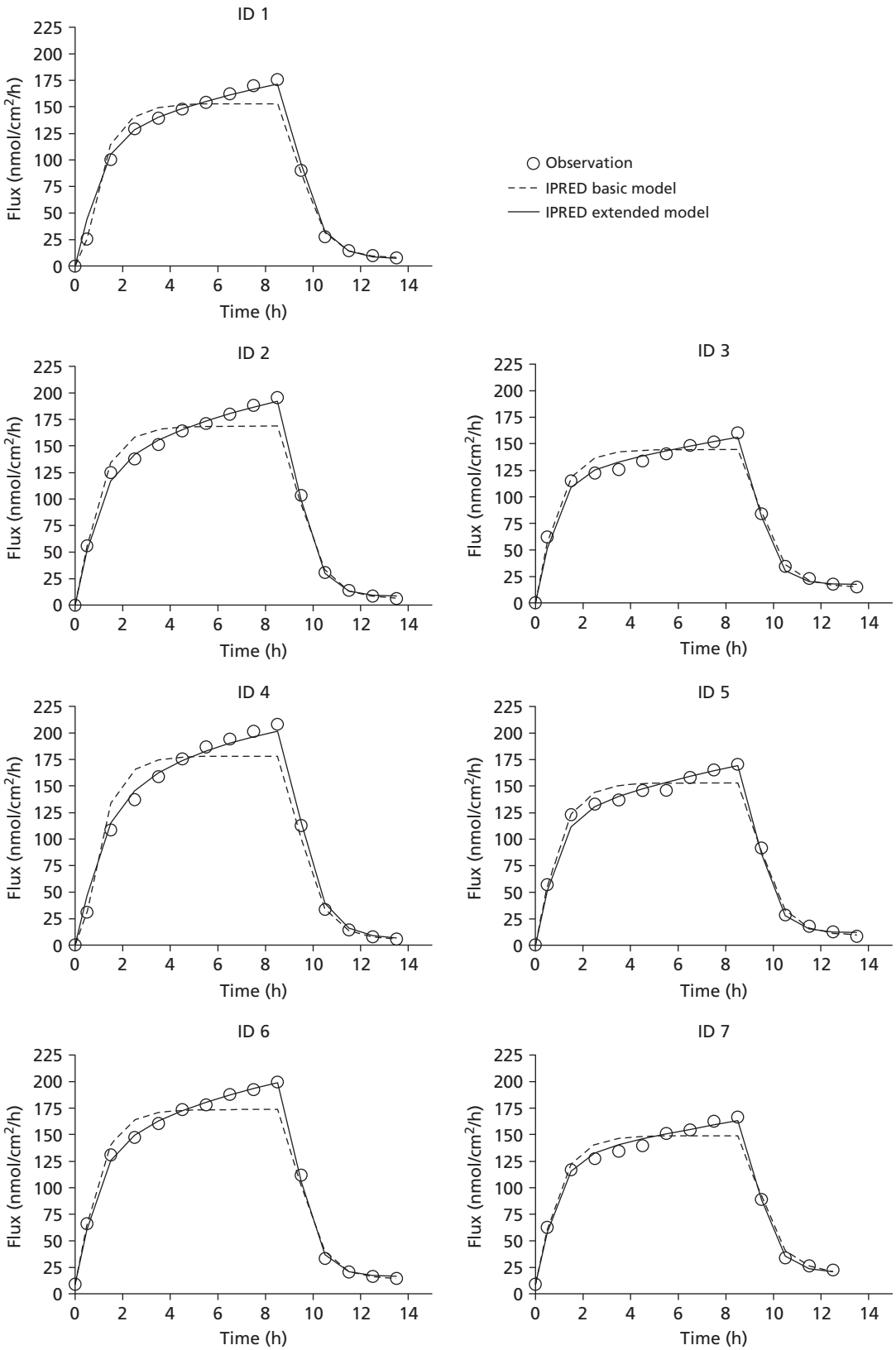

Figure 5 The individual iontophoretic flux vs time profiles of 8-OH-DPAC across human stratum corneum. Iontophoretic flux = 500 μA/cm^2. 8-OH-DPAC = 3.9 mM. The data are plotted as individual observations, together with the individual prediction (IPRED) based on the basic in-vitro model and on the extended in-vitro model with two different release constants

the reduced iontophoretic flux. Decreasing the alkyl length of one side chain on the nitrogen group from propyl (5-OH-DPAT) to ethyl (5-OH-EPAT) or further to a hydrogen (5-OH-MPAT) resulted in an increased efficiency of iontophoretic transport. This was in agreement with the observations by Del Terzo *et al.*,[29] who obtained a similar result with ionized n-alkanoic acids.

Transport pathways

In the literature different iontophoretic transport routes have been proposed: the transport route across the appendageal structures, such as hair follicles and sweat glands; and the transport route via the intercellular route in the skin.[44–47] In agreement, fitting the iontophoretic flux using a model with two release constants also suggested the presence of at least two different transport routes across human skin during current application. In the initial time period of iontophoresis transport across the more permeable pores, possibly the appendages, with a faster release to the acceptor phase (described by K_{R2}) was the major contributor to the total iontophoretic flux. However, when the iontophoresis proceeded, the contribution of the second penetration route, suggested as the intercellular pathway, with a slower release (described by K_{R1}) increased. This resulted in an increase in the total iontophoretic flux (Figure 5). Modelling transport across human stratum corneum and dermatomed skin post iontophoresis revealed that the release from the skin was best described by K_{R2}. This suggested that the appendageal route post-iontophoresis was still the predominant route. Similar observations by Turner and Guy[47] reported that the predominant transport route for the ionized calcein after iontophoresis pretreatment was via the pores.

Comparing the skin release constant K_{R2} for human stratum corneum and dermatomed skin transport, it was observed that K_{R2} was smaller during transport across dermatomed skin (Table 3). This could at least partly be attributed to the presence of hydrophilic regions and negative charged cell membranes at pH 7.4 in both the epidermis and the upper part of the dermis, slowing down the partitioning of the compounds from the skin to the acceptor phase.

Physicochemical considerations for iontophoretic delivery

In the literature several in-vitro methods have been proposed as first screening methods for transdermal iontophoretic delivery. The molecular descriptors for iontophoresis in these methods were charge, molecular weight/volume and ionic/electrophoretic mobility.[28,33,48,49]

As the electrophoretic mobility was reported as a good descriptor for the EM-flux, in this study, the EM-flux after 9 h of iontophoresis was calculated using equation 2.[28,33] The passive flux was considered to be negligible. For the transport studies across stratum corneum the EM-flux correlated linearly with the electrophoretic mobility ($R^2 = 0.85$) (Figure 6c).

Although capillary electrophoresis to estimate the EM-flux at 9 h was a good screening method for transdermal iontophoresis, this single end-point approach had some limitations. Firstly, this approach assumed that the end-point was representative for the entire iontophoretic flux, also before and after this point. However, it did not account for the shape of the curve. Secondly, it was also important to understand the influence of the physicochemical properties on the different transport parameters, such as the zero-order mass input and the release constants. This information was important to make a realistic extrapolation towards *in vivo*. The iontophoretic mass transfer was driven by a potential gradient. This implied that besides the current density and the

Table 3 The parameter estimates of data fitting the in-vitro iontophoretic delivery across human stratum corneum and dermatomed human skin of various 2-aminotetralins and chromanamine-based dopamine agonists

Skin type	Compound		I_0/S (nmol/cm²/h)		K_{R1} (slow) (/h)		K_{R2} (fast) (/h)		*Pass* (nmol/cm²/h)		*Tlag* (h)	
		n	Mean	SE	Mean	SE	Mean	SE	Mean	SE	Mean	SE
Human stratum corneum	5-OH-EPAT	6	176.56	9.33	0.06	0.02	1.43	0.13	3.17	0.58	ND	
	5-OH-MPAT	5	178.13	6.36	0.02	0.02	1.63	0.09	3.33	0.23	ND	
	5,6-di-OH-MPAT	5	133.28	5.11	ND		1.38	0.23	ND		0.08	0.13
	5,6-di-OH-DPAT	5	91.25	1.86	0.43	0.12	1.19	0.07	2.77	1.28	0.06	0.05
	8-OH-DPAC	7	113.91	2.55	0.09	0.01	1.41	0.04	8.82	1.72	0.14	0.05
	5-OH-DPAT[a]	6	119.69	8.67	0.25	0.15	1.39	0.14	4.47	0.74	0.06	0.07
	Rotigotine.HCl[b]	6	45.31	0.42	0.32	0.10	0.96	0.06	20.30	0.39	ND	
Dermatomed human skin	5-OH-EPAT	6	99.22	2.25	1.27	0.69	0.46	0.04	0.02	ND	0.27	0.01
	5-OH-MPAT	7	118.91	1.49	0.47	0.11	0.54	0.04	4.64	1.32	0.26	0.08
	5,6-di-OH-DPAT	6	116.25	2.66	0.08	0.02	0.63	0.02	10.10	1.12	0.21	0.05
	8-OH-DPAC	7	101.88	1.12	0.08	0.04	0.53	0.04	ND		0.47	0.08
	5-OH-DPAT	4	95.16	1.43	0.73	0.33	0.56	0.06	5.15	2.99	0.22	0.03
	Rotigotine.HCl[b]	6	35.31	3.33	0.03	0.02	0.28	0.04	22.70	1.62	ND	

Iontophoretic delivery; 500 μA/cm^2. The intrinsic driving force corrected for the surface area (I_0/S), the skin release constants (K_{R1} and K_{R2}), the passive driving force post-iontophoresis corrected for the surface area (P_{PI}/S; *Pass*) and the lag time (*Tlag*) are depicted. The donor concentration was 3.9 mM. Results are presented as population mean ± standard error of the estimate (n = 4–7). [a,b]Data was adapted from literature.[14,40] ND, not determined because the parameter was constrained to 0.

donor composition, which were kept constant in the transport studies, the zero-order mass transfer was dependent on the electrophoretic properties of the molecule. It was observed that the zero-order mass input, corrected for the surface area (I_0/S), was linearly correlated to the electrophoretic mobility ($R^2 = 0.93$) (Figure 6a). This also meant that the steady-state flux, calculated using equation 8, could be predicted by the electrophoretic mobility.

Previous studies demonstrated that the transport efficiency decreased with increasing molecular weight.[24–26] For instance Lai and Roberts[24] considered in the ionic mobility-pore model that the logarithm of the permeability coefficient decreased linearly with increasing molecular weight. If our interpretations were correct and K_{R2} described the release during appendageal transport, it could be expected that the release from these pores into the acceptor phase was size-dependent. Plotting the fast release constant K_{R2} against the molecular weight confirmed this size dependency. The fast release constant K_{R2} was reduced linearly with increased molecular weight (Figure 6b; $R^2 = 0.90$).

Although not fully understood, the lipophilicity of the molecules could be of importance for the transport efficiency and transport pathway. For instance Jadoul *et al*.[50] showed that fentanyl, a relatively lipophilic molecule, was distributed across the whole human stratum corneum, while the more hydrophilic thyrotropin releasing hormone was mainly localized in the pores after iontophoresis. In analogy, our observations showed that the relative contribution of the two different transport pathways was dependent on the lipophilicity of the solute. For the more lipophilic compounds, rotigotine and 5-OH-DPAT, a relatively high K_{R1} value was observed, while for the more hydrophilic compounds K_{R1} remained small. For the most hydrophilic compound, 5,6-di-OH-MPAT, even a negligible value for K_{R1} was observed. An exception was made for 5,6-di-OH-DPAT, since other mechanisms played a role in its iontophoretic transport.

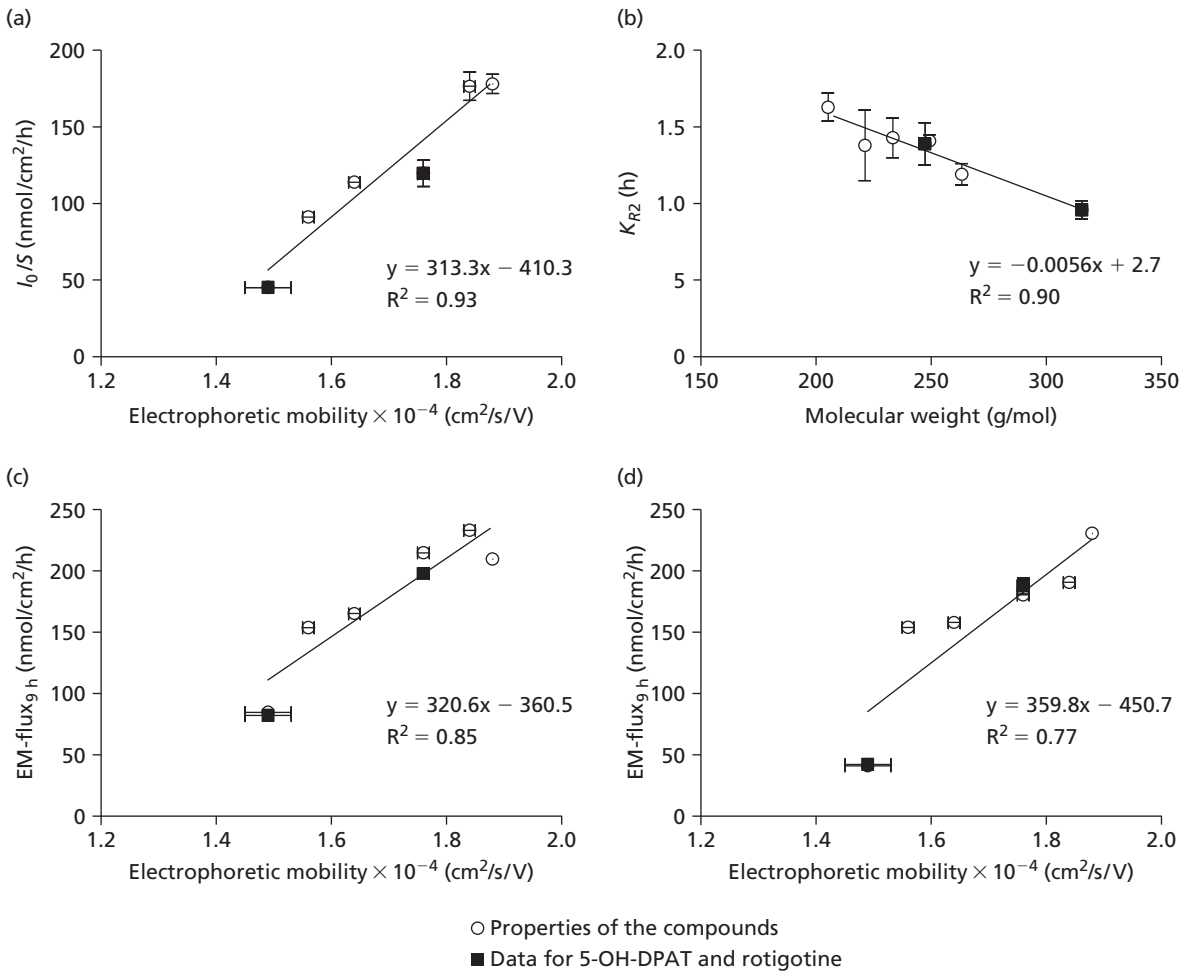

Figure 6 The relationships between the physicochemical properties of the compounds and the transport parameters. The data of 5-OH-DPAT and rotigotine were added to the graphs and included in the correlations. In all cases the donor concentration of the dopamine agonist was 3.9 mM. Data are presented as mean ± SD for the electromigrative flux (EM-flux) and electrophoretic mobilty ($n \geq 3$). The parameter estimates (I_0 and K_{R2}) are presented as mean ± standard error of the estimate ($n \geq 4$). The regression analysis was performed with the mean point estimates. (a) The linear correlation between the intrinsic driving force corrected for the surface area (I_0/S) vs the electrophoretic mobility. (b) The linear correlation between the K_{R2} and the molecular weight. (c) The EM-flux at 9 h across human stratum corneum is plotted against the electrophoretic mobility. (d) The correlation between the flux at 9 h across dermatomed human skin vs the mean electrophoretic mobility

Due to the increased membrane complexity of dermatomed human skin, the aforementioned relationships between the physicochemical properties (electrophoretic mobility, molecular weight, clogP) and the transport parameters (EM-flux, I_0/S, K_{R2}, K_{R1}) were not so evident, contrasting the observations for transport across human stratum corneum. For instance across dermatomed skin, assuming that the relative electromigrative contribution was similar to that across stratum corneum, the linear correlation between the EM-flux and the electrophoretic mobility was not so clear (Figure 6d) (R^2 = 0.78). Dermatomed human skin includes the stratum corneum, the viable epidermis and a part of the dermis, and therefore the complexity of the transport membrane is augmented. Further research is necessary to fully understand the underlying transport mechanisms involved in epidermal transport. A larger set of molecules, covering a broader range of electrophoretic mobilities presumably would increase the predictive value of capillary electro-phoresis for the EM-flux across dermatomed skin, as was observed for a series of dipeptides.[28,33] These dipeptides were grouped in three clusters, where the correlation within the groups was far less than the overall correlation, including all 11 peptides. Nonetheless the electrophoretic mobility and the corresponding EM-flux across dermatomed human skin, observed for the dopamine agonists in this study, were similar to the values obtained for the dipeptides at pH 7.4.[28,33]

Next to identifying the physicochemical-transport parameter relationships, compartmental modelling can be very useful for extrapolation towards the in-vivo situation. Assuming transport across human stratum corneum *in vitro* is representative for transport *in vivo* in humans, combining these transport parameters with pharmacokinetic parameters, applying nonlinear mixed effect modelling, simulations could be made of the iontophoretic flux *in vivo*. Nugroho *et al.*[16] demonstrated that for transdermal iontophoresis such an extrapolation from in-vitro to in-vivo was possible in rats, predicting the plasma concentration and even the pharmacodynamic effect.

Conclusions

This study has shown that small structural changes affect the solubility, electrophoretic mobility, the iontophoretic delivery efficiency and the contribution of the transport route during iontophoresis. Increasing the hydrophilicity by addition of an extra OH-group on the phenyl ring (5,6-di-OH-MPAT and 5,6-di-OH-DPAT) did not result in an increase in solubility nor transport efficiency. On the other hand solubility and iontophoretic transport could benefit from reduction in the alkyl groups at the nitrogen. In addition the electrophoretic mobility and the molecular weight can be applied to estimate the zero-order mass input I_0/S and K_{R2}, respectively. The clogP might be helpful in determination of the relative contribution of the different transport pathways by estimation of K_{R1}, although further research is required to define a clear relationship. With the estimated parameters, using the proposed compartmental model, it will be possible to simulate the iontophoretic flux profile across human stratum corneum *in vitro*. Simulations can be a helpful tool in designing future experiments, giving the opportunity to explore different flux profiles and different study designs.

Declarations

Conflict of interest

The Author(s) declare(s) that they have no conflicts of interest to disclose.

Funding

This research was financially supported by a grant (LKG 6507) of the Dutch Technology Foundation STW, Utrecht, The Netherlands.

References

1. Sage BH. Iontophoresis. In: Smith EW, Maibach HI, eds. *Percutaneous Penetration Enhancers*. Boca Raton: CRC Press Inc., 1995: 351–365.
2. Nutt JG. Continuous dopaminergic stimulation: is it the answer to the motor complications of Levodopa? *Mov Disord* 2007; 22: 1–9.
3. Olanow CW. The scientific basis for the current treatment of Parkinson's disease. *Annu Rev Med* 2004; 55: 41–60.
4. Olanow CW *et al*. The scientific and clinical basis for the treatment of Parkinson disease (2009). *Neurology* 2009; 72: S1–36.
5. van Laar T *et al*. Stepwise intravenous infusion of apomorphine to determine the therapeutic window in patients with Parkinson's disease. *Clin Neuropharmacol* 1998; 21: 152–158.
6. Tugwell C. *Parkinson's disease in focus*. London: Pharmaceutical Press; 2008.
7. van der Geest R *et al*. Iontophoretic delivery of apomorphine. I: In vitro optimization and validation. *Pharm Res* 1997; 14: 1798–1803.
8. van der Geest R *et al*. Iontophoretic delivery of apomorphine. II: An in vivo study in patients with Parkinson's disease. *Pharm Res* 1997; 14: 1804–1810.
9. Li GL *et al*. Transdermal iontophoretic delivery of apomorphine in patients improved by surfactant formulation pretreatment. *J Control Release* 2005; 101: 199–208.
10. Li GL *et al*. Iontophoretic R-apomorphine delivery in combination with surfactant pretreatment: in vitro validation studies. *Int J Pharm* 2003; 266: 61–68.
11. Luzardo-Alvarez A *et al*. Iontophoretic delivery of ropinirole hydrochloride: effect of current density and vehicle formulation. *Pharm Res* 2001; 18: 1714–1720.
12. Luzardo-Alvarez A *et al*. In vivo iontophoretic administration of ropinirole hydrochloride. *J Pharm Sci* 2003; 92: 2441–2448.
13. Nugroho AK *et al*. Transdermal iontophoresis of rotigotine: influence of concentration, temperature and current density in human skin in vitro. *J Control Release* 2004; 96: 159–167.
14. Nugroho AK *et al*. Transdermal iontophoresis of rotigotine across human stratum corneum in vitro: influence of pH and NaCl concentration. *Pharm Res* 2004; 21: 844–850.
15. Nugroho AK *et al*. Transdermal iontophoresis of the dopamine agonist 5-OH-DPAT in human skin in vitro. *J Control Release* 2005; 103: 393–403.
16. Nugroho AK *et al*. Pharmacokinetics and pharmacodynamics analysis of transdermal iontophoresis of 5-OH-DPAT in rats: in vitro-in vivo correlation. *J Pharm Sci* 2006; 95: 1570–1585.
17. Beart PM *et al*. Radioreceptor binding reveals the potencies of N,N-disubstituted 2-aminotetralins as D2 dopamine agonists. *Naunyn Schmiedebergs Arch Pharmacol* 1987; 336: 487–493.

18. Beaulieu M *et al*. N,N-disubstituted 2-aminotetralins are potent D-2 dopamine receptor agonists. *Eur J Pharmacol* 1984; 105: 15–21.
19. Hacksell U *et al*. N-Alkylated 2-aminotetralins: central dopamine-receptor stimulating activity. *J Med Chem* 1979; 22: 1469–1475.
20. Horn AS *et al*. Synthesis and dopaminergic activity of a new oxygen isostere of the 2-aminotetralins: N,N-dipropyl-8-hydroxy-3-chromanamine. *Eur J Med Chem* 1988; 22: 325–328.
21. Thorberg SO *et al*. Aminochromans: potent agonists at central dopamine and serotonin receptors. *Acta Pharm Suec* 1987; 24: 169–182.
22. van Vliet LA *et al*. Affinity for dopamine D2, D3, and D4 receptors of 2-aminotetralins. Relevance of D2 agonist binding for determination of receptor subtype selectivity. *J Med Chem* 1996; 39: 4233–4237.
23. Vermue NA *et al*. Pharmacological profile of N,N dipropyl-8-hydroxy-3-chromanamine, an oxygen isostere of the dopamine agonist N,N dipropyl-5-hydroxy-2-aminotetralin with enhanced presynaptic selectivity. *Arch Int Pharmacodyn Ther* 1988; 293: 37–56.
24. Lai PM, Roberts MS. An analysis of solute structure-human epidermal transport relationships in epidermal iontophoresis using the ionic mobility: pore model. *J Control Release* 1999; 58: 323–333.
25. Roberts MS *et al*. Epidermal iontophoresis: I. Development of the ionic-mobility pore model. *Pharm Res* 1998; 15: 1569–1578.
26. Yoshida NH, Roberts MS. Solute molecular size and transdermal iontophoresis across excised human skin. *Control Release* 1993; 25: 177–195.
27. Abla N *et al*. Effect of charge and molecular weight on transdermal peptide delivery by iontophoresis. *Pharm Res* 2005; 22: 2069–2078.
28. Abla N *et al*. Capillary zone electrophoresis for the estimation of transdermal iontophoretic mobility. *J Pharm Sci* 2005; 94: 2667–2675.
29. Del Terzo S *et al*. Iontophoretic transport of a homologous series of ionized and nonionized model compounds: influence of hydrophobicity and mechanistic interpretation. *Pharm Res* 1989; 6: 85–90.
30. Schuetz YB *et al*. Structure-permeation relationships for the non-invasive transdermal delivery of cationic peptides by iontophoresis. *Eur J Pharm Sci* 2006; 29: 53–59.
31. Nugroho AK *et al*. Compartmental modeling of transdermal iontophoretic transport: I. In vitro model derivation and application. *Pharm Res* 2004; 21: 1974–1984.
32. Nugroho AK *et al*. Compartmental modeling of transdermal iontophoretic transport II: in vivo model derivation and application. *Pharm Res* 2005; 22: 335–346.
33. Henchoz Y *et al*. A fast screening strategy for characterizing peptide delivery by transdermal iontophoresis. *J Control Release* 2009; 137: 123–129.
34. Poole SK *et al*. Determination of acid dissociation constants by capillary electrophoresis. *J Chromatogr A* 2004; 1037: 445–454.
35. Wan H *et al*. Rapid screening of pKa values of pharmaceuticals by pressure-assisted capillary electrophoresis combined with short-end injection. *J Chromatogr A* 2002; 979: 369–377.
36. Holford N. The Visual Predictive Check-Superiority to Standard Diagnostic (Rorschach) Plots. *PAGE 14, Abstr 738 [wwwpage-meetingorg/?abstract=738]* 2005.
37. Tetko IV, Bruneau P. Application of ALOGPS to predict 1-octanol/water distribution coefficients, logP, and logD, of AstraZeneca in-house database. *J Pharm Sci* 2004; 93: 3103–3110.
38. Tetko IV *et al*. Virtual computational chemistry laboratory–design and description. *J Comput Aided Mol Des* 2005; 19: 453–463.
39. VCCLAB. Virtual Computational Chemistry Laboratory, http://www.vcclab.org. 2005.
40. Ackaert OW *et al*. Mechanistic studies of the transdermal iontophoretic delivery of 5-OH-DPAT in vitro. *J Pharm Sci*; 99: 275–285.
41. Cheng HY *et al*. Electrochemical studies of the oxidation pathways of apomorphine. *Anal Chem* 1979; 51: 2243–2246.
42. Afkhami A *et al*. Kinetic study of the oxidation of some catecholamines by digital simulation of cyclic voltammograms. *Int J Chemical Kinetics* 2005; 37: 17–24.
43. Peck KD *et al*. Quantitative description of the effect of molecular size upon electroosmotic flux enhancement during iontophoresis for a synthetic membrane and human epidermal membrane. *J Pharm Sci* 1996; 85: 781–788.
44. Alvarez-Roman R *et al*. Visualization of skin penetration using confocal laser scanning microscopy. *Eur J Pharm Biopharm* 2004; 58: 301–316.
45. Barry W, ed. *Dermatological Formulations. Percutaneous Absorption.* New York: Marcel Dekker; 1983.
46. Cullander C. What are the pathways of iontophoretic current flow through mammalian skin? *Adv Drug Deliv Rev* 1992; 9: 119–135.
47. Turner N, Guy RH. Iontophoretic transport pathways: dependence on penetration physicochemical properties. *J Pharm Sci* 1997; 86: 1385–1389.
48. Mudry B *et al*. Quantitative structure-permeation relationship for iontophoretic transport across the skin. *J Control Release* 2007; 122: 165–172.
49. Yoshida NH, Roberts MS. Prediction of cathodal iontophoretic transport of various anions across excised skin from different vehicles using conductivity measurements. *J Pharm Pharmacol* 1995; 47: 883–890.
50. Jadoul A *et al*. Quantification and localization of fentanyl and TRH delivered by iontophoresis in the skin. *Int J Pharmaceutics* 1995; 120: 221–228.